Promote and Ensure the Quality of Welding Education in the Region

March 20th-22th, 2019

Queen Sirikit National Convention Centre (QSNCC), Bangkok, Thailand

IIWAP 2019 E-Proceeding Book

The 8th Asia Pacific IIW International Congress

Hosted by WELDING INSTITUTE THAILAND

Supported by

Organized by NCC

Sponsored by

Partners

The Influence of Laser Parameters on the Melted Track and Microstructure of AISI 316L Fabricated by L-PBF Process

P. Ninpetch[1], N. Teenok[2], P. Kowitwarangkul[1,*], S. Mahathanabodee[2], R. Tongsri[3], P. Ratanadecho[4]

[1] The Sirindhorn International Thai-German Graduate School of Engineering (TGGS), King Mongkut's University of Technology North Bangkok (KMUTNB), Bangkok, Thailand

[2] Department Production Engineering, Faculty of Engineering,King Mongkut's University of Technology North Bangkok (KMUTNB), Bangkok, Thailand

[3] Particulate Materials Processing Technology Laboratory (PMPT), National Metal and Materials Technology Center, Pathum Thani, Thailand

[4] Department of Mechanical Engineering, the Faculty of Engineering, Thammasat University (Rangsit Campus), Pathum Thani, Thailand

*Corresponding author's email address: pruet.k@tggs.kmutnb.ac.th

Abstract

Laser powder bed fusion process (L-PBF) is the most widespread additive manufacturing (AM) process which uses laser source scanning as a moving heat source on powder bed to fully melt the metal powder in a layer-by-layer fashion. During the process, it involves various complex multiphysics such as materials absorption, heat transfer, molten fluid flow, phase transformation etc. These physical phenomena have significant effect on physical properties, mechanical properties and the microstructure of final parts. The present study aims to investigate the influence of laser parameters including scanning speed and hatch spacing (distance between laser scanning track) on the laser melted track width, layer formation, microstructure and microhardness of AISI 316L stainless steel fabricated by Laser powder bed fusion (L-PBF) process with low laser power (Max. 50W). The experimental results presented that the laser melted track width is decreased from 250 to 150 micron when the scanning speed is increased from 5 to 15 mm/s. The discontinuous melted track with balling effect can be observed in the layer formation at the scanning speed of 5 mm/s. When the scanning speed is increased to 10 mm/s, more continuous laser melted track was formed. The microstructure of AISI 316L stainless steel fabricated by L-PBF process consists of cellular columnar structure and dendrite structure oriented according to temperature gradient direction during rapid cooling.

Keywords: *Additive manufacturing, Laser powder bed fusion, Melted track, Microstructure*

Introduction

Laser powder bed fusion process (L-PBF) is the most widespread additive manufacturing (AM) process which uses laser source scanning as a moving heat source on powder bed to fully melt the metal powder in a layer-by-layer fashion. The schematic of laser powder bed fusion process is shown in Figure 1. The main process parameters consist of laser power, laser spot diameter, scanning speed, hatch spacing, scan strategy, overlap rate, layer thickness and working atmosphere [1]. During the process, it involves various complex multiphysics such as materials absorption, heat transfer, molten fluid flow, phase transformation, rapid melting, rapid solidification, recoil pressure and chemical reaction, etc [2]. These physical phenomena have significant effect on physical properties, mechanical properties and the microstructural evolution of final parts, e.g. density, dimension, void, porosity, non-fully melted particle, and balling effect phenomena [2].

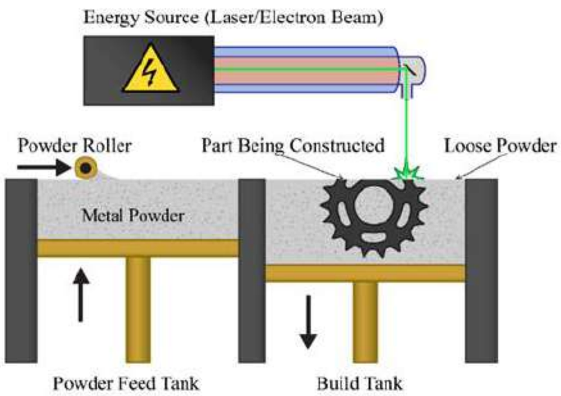

Figure 1 The schematic of laser powder bed fusion (L-PBF) process [3]

L-PBF process is widely used for metallic materials, being already used with success in different industrial applications such as jig-fixture, mold tooling, biomedical parts, automotive parts, aerospace parts and jewelry [4]-[5]. The process can precisely produce fully dense metallic parts from metal alloys, e.g. titanium alloys, inconel alloys, cobalt chrome, aluminium alloys, stainless steels, and tool steels [6]. This study focuses on AISI 316L stainless steel. The AISI 316L is a type of austenitic stainless steel, which main containing alloys 16-18%wt Cr and 10-14%wt Ni. It has excellent corrosion resistance, good weldability and good formability [7]. I. Yadroitsev and I. Smurov studied the effect of process parameters such as laser power, scanning speed and layer thickness on the laser tracks formation of AISI 316L. It was found that the stability zones occur when the laser melted track is continuous and instability zone can be formed when the tracks are not continuous [8]. Y. GUO et al. testified the laser melted tracks and layer formation in selective laser melting of niobium solid solution alloy. The results show that the continuous of single track could be appeared by using the proper laser power and scanning speed. The width and depth of laser melted track is increased with an increase of the laser beam energy density [9]. R. Li et al. studied the effect of scanning speed on balling behaviour of AISI 316L. They found that the laser scanning track widths are narrowed gradually when the scanning speed is increased [10]. I. Yadroitsev and I. Smurov investigated the effect of hatch distance on surface morphology during selective laser melting. The process parameters used in the study were laser power with 50 W and the scanning speed with 0.14 m/s. The varied hatch spacing are from 60 up to 280 μm with a step of 20 μm. They summarized that the aperture between two neighbouring tracks is increased and leads to separation with an increase of hatch spacing [11]. J.A. Cherry et al. investigated the effect of process parameters on the microstructural and mechanical properties of 316L stainless steel parts by selective laser melting. The results reveal that the hardness of material increases when the porosity is decreased [12]. V. Sufiiarov et al. studied the selective laser melting process of AISI 316L powder. The results from the study show that the laser powder bed fusion process can produce parts with higher mechanical properties than conventional manufacturer [13]. Z. Brytan reported the comparisons of vacuum sintered with selective laser melting (SLM) process of AISI 316L stainless steel. The results present that applications of selective laser melting (SLM) makes it possible to double increase the mechanical properties of components manufactured from austenitic stainless steel type AISI 316L compared to sintering in a vacuum. The microstructure from L-PBF process generally consists of overlapped melted pool tracks with crystallised grains of cellular-columnar structure oriented according to thermal gradient direction. The cellular-columnar microstructure is typical for stainless steel solidified under rapid cooling rate and rapid solidification [14].

The present study aims to investigate the influence of laser process parameters including scanning speed and hatch spacing (distance between laser scanning track) on the melted track width, layer formation, microstructure and microhardness of AISI 316L stainless steel fabricated by Laser powder bed fusion (L-PBF) process with low laser power. The results obtain from this study will be useful for the further research studies in metal 3D printing process in the coming future of the fourth industrial revolution in Thailand.

Experimental procedure

Material

The materials used in this experiment was AISI 316L stainless steel spherical shaped powder which is particularly used in additive manufacturing process from Hoganas, Belguim S.A factory with the metal powder size of 20-53 μm as shown in Figure 2. The chemical compositions of AISI 316L stainless steel are shown in Table 1 [15].

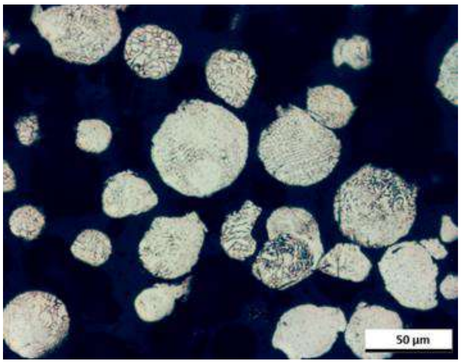

Figure 2 AISI 316L stainless steel spherical-shaped powder

Table 1 The chemical compositions of AISI 316L stainless steel

Chemical composition (% wt)							
C	Mn	Si	P	S	Cr	Mo	Ni
0.03	2	1	0.04	0.01	18	3	14

Processing

The building platform and gas chamber in the L-PBF system were designed and built to create the specimens to investigate the microstructure, melted track and microhardness of AISI 316L stainless steel fabricated by L-PBF process as shown in Figure 3. The laser energy source with continuous wave (CW) mode, JenLas® fiber ns 50, at Center Innovation of Design and Engineering for Manufacturing (Col-DEM), KMUTNB which has maximum power of 50 Watts was used as heat energy to fully melt the metal powder bed layer by layer. The laser focus position and the diameter of laser spot, used in this experiment are 18 cm and 0.03 mm respectively. This experiment was conducted in an argon inert atmosphere. The experiment procedure started with creating the metal powder bed to define the layer thickness of the specimen. After that the metal powder was raked by the recoater on the work space to create metal powder bed. Then, the laser energy source with continuous wave (CW) mode was used as heat energy to fully melt the metal powder bed to create the metal powder layer formation.

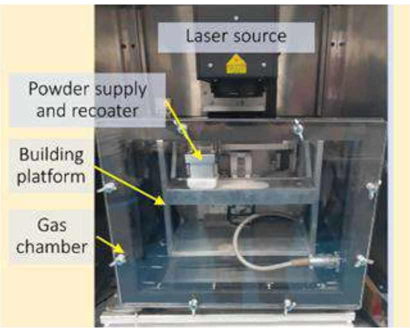

Figure 3 The building platform and gas chamber in the L-PBF process

Material Characterization

The optical macroscope was used to analyse the laser melted track width and layer formation of the AISI 316L stainless steel fabricated by L-PBF process. The microstructure of the AISI 316L stainless steel fabricated by L-PBF process was characterized by the optical microscope (OM). In the characterized process, the specimens were grinded with sand paper from coarse grit to fine grit (500 to 2000) step by step to make the surface smooth and flat. After the grinding process, the specimens were polished on the polishing paper with the alumina powder suspension 0.3 and 0.1 micron to make the polishing surface. Then, the specimens were etched by acid. The acids used in this process were mixed by nitric acid (HNO_3), glycerol ($C_3H_8O_3$) and hydrochloric acid (HCl) with a ratio of 1:2:3. The Scanning electron microscope machine with energy dispersive spectroscopy technique (SEM/EDS) technique was used to characterize the structure of the material and to investigate the main chemical composition of specimens. The micro hardness of AISI 316L stainless steel fabricated by L-PBF process were carried out by measuring the Vickers hardness along the cross-section area of the specimens. The applied test load used in the test was 100-gram force (gf).

The details of process parameters for the case studies in the experiment are shown in Table 2. The laser power, scanning speed, layer thickness and hatch spacing used in the experiment are 50 watt, 5 mm/s, 10 mm/s, 15 mm/s, 50 and 300 µm respectively.

Table 2 The experimental study case with different process parameter

Cases	Scanning speed (mm/s)	Hatch spacing (mm)	Layer thickness (µm)
1	5	0.3	50
2	10	0.3	50
3	15	0.3	50
4	5	0.1	300
5	5	0.3	300
6	5	0.5	300

Experimental results and Discussion

Effect of Scanning Speed on Laser Melted Track Width

Figure 4 shows the influence of scanning speed on laser melted track width. The laser melted track width varies between 149 and 252 µm. The result presents that the laser melted track width is decreased when the scanning speed is increased due to the thermal condition which has lower heat accumulation in the metal powder bed of L-PBF process. This result is in agreement with the previous research study [16]. The laser melted track width has a significant effect on determining the overlap rate of hatch spacing to produce the fully dense parts.

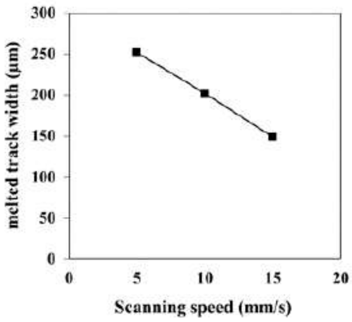

Figure 4 The laser melted track width with different scanning speed

Layer formation with different laser parameters

The layer formation with different hatch spacing (0.1 mm (a) 0.3 mm (b) and 0.5 mm (c)) is shown in Figure 5. At H = 0.1 mm, the discontinuous melted tracks with balling effect were appeared due to oxidation reaction and the insufficient laser heat energy to fully melt the metal powder as shown in Figure 5 (a). The pores can be seen inside the layer formation. When increasing the hatch spacing to 0.3 mm, the discontinuous melted track with balling effect can be observed with the reduced balling size as shown in Figure 5 (b). Also, the pore fraction inside the layer was reduced. At H= 0.5 mm, the discontinuous melting track with fragment was observed and the laser melted track is arranged along laser scan pattern as shown in Figure 5 (c). In L-PBF process the hatch spacing is the significant process parameter that provide the good quality of products with less porosity. Figure 6 illustrates the layer formation with different scanning speed, 5 mm/s (a), 10 mm/s (b) and 15 mm/s (c). It was discovered that the discontinuous with fragment and instability of laser melted track occur at the scanning speed of 5 mm/s. When the scanning speed is increased to 10 mm/s, more continuous laser melted track was formed. At the scanning speed of 15 mm/s, the laser melted track cannot be completely melted. The pore from separated particles of metal powder inside the layer formation can be found due to insufficient laser energy density. The continuous melt track can be presented when the properly process parameters are applied.

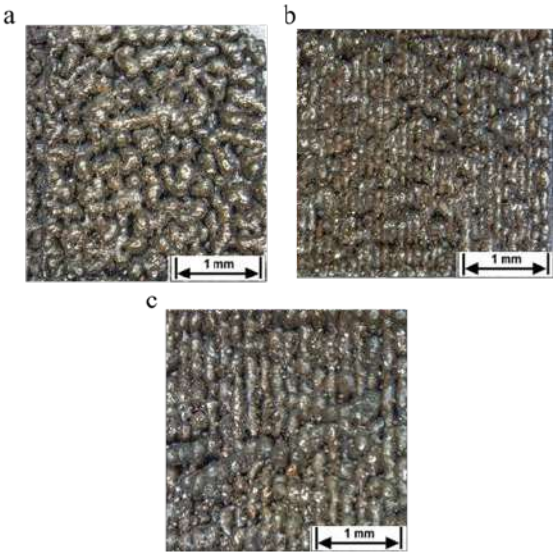

Figure 5 The layer formation with different hatch spacing, (a) H = 0.1 mm, (b) H = 0.3 mm, (c) H = 0.5 mm

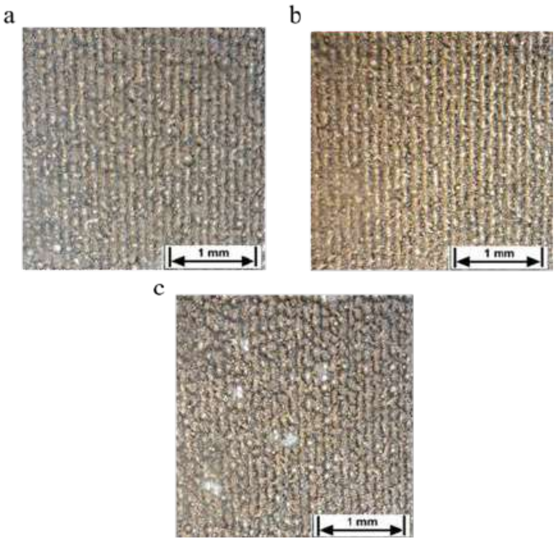

Figure 6 The layer formation with different scanning speed, (a) v = 5 mm/s, (b) 10 mm/s and (c) 15 mm/s

Microstructure of AISI 316L stainless steel fabricated by L-PBF process

In L-PBF, the rapid melting and rapid solidification can occur with the microstructural evolution process. Figure 7 (a) shows the cross-section area of AISI 316L melted particle from case 1. The particle shown in this Figure is the one that has large size due to the balling effect. The microstructure of AISI 316L stainless steel fabricated by L-PBF process consists of cellular columnar structure and dendrite structure oriented according to temperature gradient direction during rapid cooling as shown in Figure 7 (b). In the L-PBF, the cellular-columnar structure can be formed due to the sufficiency of the ratio of temperature gradient and growth rate (G/R) values. The cellular-columnar structure is a typical microstructure of AISI 316L stainless steel with rapid solidification [14]. The chemical compositions of the 316L stainless steel obtained by scanning electron microscope with EDS technique is presented in Figure 8. The main alloying element found in AISI 316L are Cr, Ni and Mo.

Figure 7 Cross section area of melted powder bed layer formation (a), Microstructure of AISI 316L powder fabricated by L-PBF process

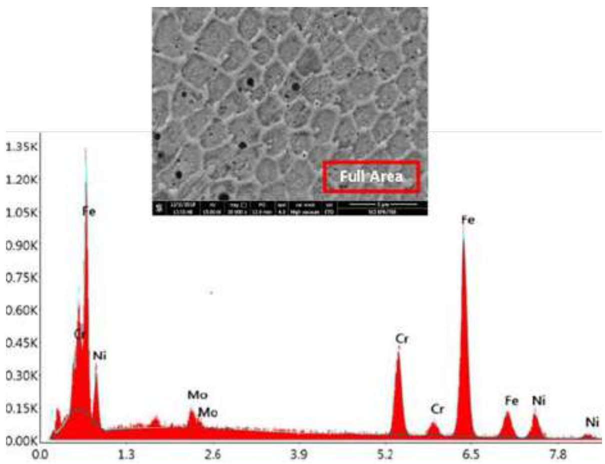

Figure 8 The chemical composition of the cellular structure obtained by SEM-EDS

Effect of Scanning Speed and Hatch Spacing on Cellular Structure

The cellular structure of AISI 316L with different process parameters are shown in Figure 9 and 10. The result revealed that the size of cell spacing is decreased with an increase of scanning speed from 5 mm/s to 10 mm/s and 15 mm/s due to higher cooling rate of materials under solidification process as shown in Figure 9. The results from this experimental study are in agreement with previous research [19]. Figure10 shows the cellular structure with different hatch spacing (0.1 mm, 0.3mm and 0.5 mm). The experimental result presented that the higher the hatch spacing is, the lower the cell spacing size will take place.

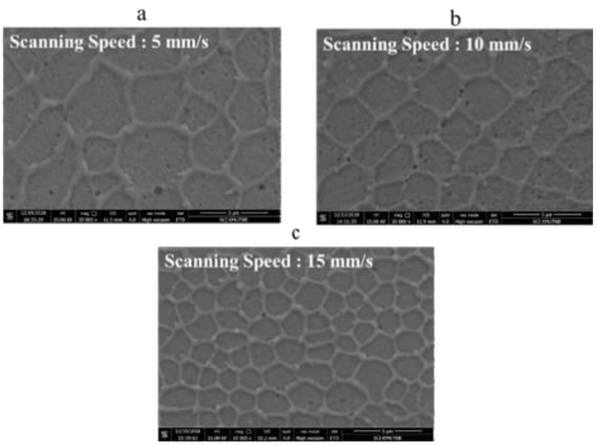

Figure 9 The cellular structure with different scanning speed

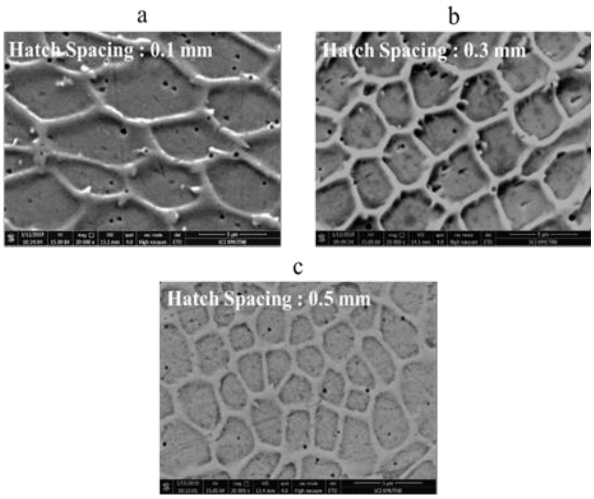

Figure 10 The cellular structure with different hatch spacing

Microhardness of AISI 316L stainless steel fabricated by L-PBF process

The microhardness of L-PBF compared with the conventional process [18-19] is presented in figure 11. The results from the study show that the laser powder bed fusion process can produce parts with higher microhardness than that of the conventional manufacturer due to the rapid cooling rate with finer grain of materials as describe in [19].

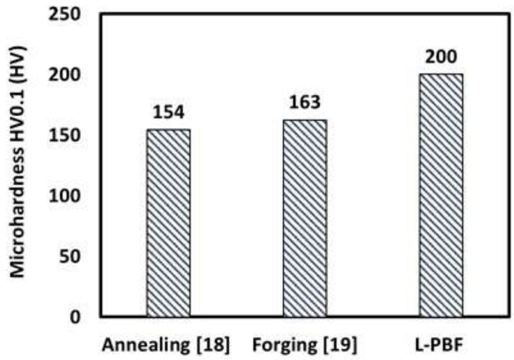

Figure 11 The microhardness of AISI 316L fabricated by L-PBF compared with the conventional process

The micro Vickers hardness of AISI 316L stainless steel fabricated by L-PBF process with different hatch spacings (0.1 mm, 0.3 mm and 0.5 mm) is shown in figure 12. The result indicated that different hatch spacings have minor effects on the microhardness of AISI 316.

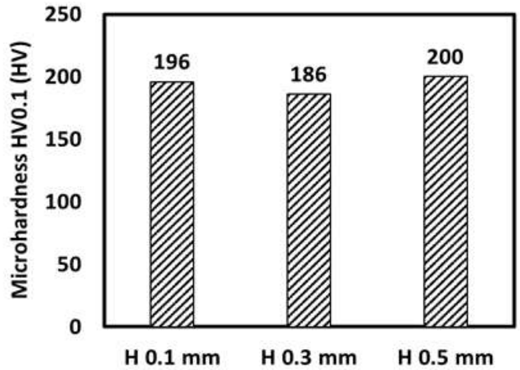

Figure 12 Microhardness of AISI 316L fabricated by L-PBF process

Conclusions

In this research, the influence of laser parameters on the laser melted track width, layer formation, microstructure and microhardness of AISI 316L stainless steel fabricated by Laser powder bed fusion (L-PBF) process with low laser power (20-50 W) was investigated. The results from the experiment are shown as follows:

1. The laser melted track width is decreased from 250 to 150 micron when the scanning speed is increased from 5 to 15 mm/s.
2. The discontinuous with fragment and instability of laser melted track occur at the scanning speed of 5 mm/s. When the scanning speed is increased to 10 mm/s, more continuous laser melted track was formed. At the scanning speed of 15 mm/s, the laser melted track cannot be completely melted. The pore from separated particles of metal powder inside the layer

formation can be found due to insufficient laser energy density.

3. The discontinuous melted tracks with balling effect were appeared at H 0.1 mm due to oxidation reaction and the insufficient laser heat energy to fully melt the metal powder. The pores can be seen inside the layer formation. When increasing the hatch spacing to 0.3 mm, the discontinuous melted track with balling effect can be observed with the reduced balling size as Also, the pore fraction inside the layer was reduced. At H= 0.5 mm, the discontinuous melting track with fragment was observed and the laser melted track is arranged along laser scan pattern.
4. The microstructure of AISI 316L stainless steel fabricated by L-PBF process consists of cellular columnar structure and dendrite structure oriented according to temperature gradient direction.
5. The size of cell spacing is decreased with an increase of scanning speed and hatch spacing.
6. The L-PBF process can produce the final parts with higher micro harness than conventional manufacturer due to rapid cooling rate and small grain size.

Acknowledgement

The authors would like to thank the fund support from Thailand Graduate Institute of Science and Technology (TGIST), National Science and Technology Development Agency (NSTDA) contract No. SCA-CO-2560-4552-TH, the Thailand Research Fund (TRF) and the Commission on Higher Education (CHE) under the TRF contract No. MRG6180164.

References

[1] Daniel, T., "The Development of Design Rules for Selective Laser Melting", Ph. D Thesis, University of Wales Institute Cardiff, 2009.

[2] Yousub, L. and W, Z., "Mesoscopic Simulation of Heat Transfer and Fluid Flow in Laser Powder Bed Additive Manufacturing", Proc. of the 26th Annual International Solid Free Form Fabrication Symposium, Austin, TX, US, August 2015, pp. 1154-1165.

[3] Matt, S., "Metal 3D Printing: Laser Sintering vs. Bulk Sintering in a Furnace – Pros and Cons", https://3dprint.com/193946/laser-sintering-vs-bulk-sintering/ [Accessed on 5 Jan 2019].

[4] T, W., "Additive Manufacturing State of the Industry", Wohlers report, 2010, pp. 1-26.

[5] Chenhao, F. and Y, B, G., "3-dimension finite element modelling of selective laser melting Ti-6AL-4V alloy", Proc. of the 25th Annual International Solid Free Form Fabrication Symposium Austin, TX, US, August. 2014, pp. 1129-1144.

[6] Valmilk, B., Prakash, K., Vinaykumar P., Kiran G., Rajkumar, S. and Sheryans, K., "A Review on Powder Bed Fusion Technology of Metal Additive Manufacturing", Proc. of the 4th International conference and exhibition on Additive Manufacturing Technologies-AM-2014 Bengaluru, India, September, 2014.

[7] Stainless Steel - Grade 316L - Properties, Fabrication and Applications (UNS S31603)., https://www.azom.com, accessed on 5 Jan 2019.

[8] Igor, Y. and I, S., "Selective laser melting technology: from the single laser melted track stability to 3D parts of complex shape", Physics Procedia, 2010, vol. 5, pp. 551-560.

[9] Yueiling G., Lina J., Bin K., Na W. and Hu Z., "Single track and single layer formation in selective laser melting of niobium solid solution alloy", Chinese Journal of Aeronautics, 2018, 31(4), pp.860-866.

[10] Rudi, L., Jinhui L., Yusheng S., Li W. and Wei J., "Balling behavior of stainless steel and nickel powder during selective laser melting process", Int J Adv Manuf Technol, 2012, vol. 59, pp. 1025-1035.

[11] Igor, Y. and I, S., "Surface Morphology in Selective Laser Melting of Metal Powders", Physics Procedia, 2011, vol. 12, pp. 264-270

[12] J, A. C., HM, D., Shahid, M., Nicholas P. L., S G. R. B. and J, S., "Investigation into the effect of process parameters on microstructural and physical properties of 316L stainless steel parts by selective laser melting", Int J Adv Manuf Technol, 2015, (76), pp. 869–879, 2015.

[13] Vadim, S., Evgenii, B., Igor, P. and Dmitry, M., "Study of microstructure and properties of 316l steel after selective laser melting", Proc. of the METAL 2016 - 25th Anniversary International Conference on Metallurgy and Material, Brno, Czech Republic, EU, May 2016, pp. 659-663.

[14] Brytan, Z., "Comparison of vacuum sintered and selective laser melted steel AISI 316L", Arch. Metall. Mater, 2017, vol.62 (4), pp. 2125-2131.

[15] AMPERPRINT® Additive Manufacturing powders Höganäs,https://www.hoganas.com/en/powder/technologies/additive-manufacturing/ [Accessed on 29 Jan 2019].

[16] Yu, C. W., Weng, S. H., Cheng, H. S., Chih, H. C. and Huey, J. L., "Parametric study of surface morphology for selective laser melting on Ti6Al4V powder bed with numerical and experimental methods, International Journal of Material Forming, 2017, pp. 1-7.

[17] Yuan, Z., "Sub-grain structure in additive manufactured stainless steel 316L", Academic dissertation for the Degree of Doctor of Philosophy in Materials chemistry, Stockholm University, 2017.

[18] Austenitic Stainless Steel Investment Cast Alloy Properties,http://www.wisconsinprecision.com/austenitic-stainless-steel-investment-castings.php [Accessed on 27 Feb 2019].

[19] Eriksson, P., "Evaluation of mechanical and microstructural properties for laser powder-bed fusion 316L", Uppsala university, 2018.